Catalysis Letters, Vol. 117, Nos. 3–4, September 2007 (© 2007)
DOI: 10.1007/s10562-007-9128-3

Zirconium sulfate supported on activated carbon as catalyst for esterification of oleic acid by *n*-butanol under solvent-free conditions

Joon Ching Juan,[a,b] Jingchang Zhang,[a,*] Yajie Jiang,[a] Weiliang Cao,[a] and Mohd Ambar Yarmo[b]

[a]*Institute of Modern Catalysis, Beijing University of Chemical Technology, State Key Laboratory of Chemical Resource Engineering, Ministry of Education, Beijing 100029, China*

[b]*Advanced Catalysis Technology Laboratory, School of Chemical Sciences and Food Technology, Faculty of Science and Technology, Universiti Kebangsaan Malaysia, Bangi 43600, Malaysia*

Received 16 April 2007; accepted 17 April 2007

It has been shown that the activated carbon-supported zirconium sulfate (ZS) is an efficient solid catalyst for the esterification of oleic acid by *n*-butanol under solvent-free condition. The effect of mole ratio of the reactant, time and catalyst loading on the conversion was examined. The correlation among XRD, nitrogen adsorption data and catalytic activity suggested that ZS has been finely dispersed on activated carbon, which are active in the esterification of oleic acid. The reaction shows that the supported ZS exhibits a higher activity than that of parent ZS and conventional resins.

KEY WORDS: zirconium sulfate; activated carbon; esterification; oleic acid.

1. Introduction

Fatty acid esters are used as raw materials for emulsifiers or as oiling agents for foods, spin finishes and textiles; lubricants for plastics; paints and ink additives and for mechanical processing; personal care emollients; surfactants and base materials for perfumes, etc. [1]. They also used as solvents, co-solvents, and oil carriers in agricultural industry [1]. They are produced conventionally by the esterification of fatty acids with alcohols. Esterification is usually catalyzed by an acid catalyst donor of protons, such as sulfuric acid, para-toulene sulfonic acid or phosphoric acid [2]. However, these acid catalysts are toxic, corrosive, and hard to remove from the reaction medium [3]. Therefore, the challenge was to replace them by solid acid catalyst, such as zeolites, alumina or resins, which are easier to separate from the products and less toxic.

Recently, Cao *et al*. [4,5] have used zirconium sulfate (ZS) for esterification of short chain carboxylic acids. They successfully obtained good product selectivity with high catalytic activity using ZS. In general, ZS has low toxicity (LD_{50} = 3500 mg kg^{-1}) and shows no evidence of carcinogenicity. Therefore, ZS has attracted great interest as potential green catalyst because green catalysts require not only high catalytic activity and atom efficiency, but also low toxicity, low cost and ease of handling. Unfortunately, ZS partially soluble in water (525 gL^{-1}), it is often difficult to separate them from the reaction products. Besides that, ZS owed a low surface area (5–11 m^2 g^{-1}). Therefore, a new family of catalysts has been developed by supporting ZS on various supports [6]. Activated carbon is useful support for catalysts, especially the use as carrier for noble metals has been studied extensively [7]. Carbon-supported noble metal catalysts find broad application in hydrogenation of intermediates and fine chemicals. In addition, they also used as support for inorganic salt, such as heteropoly acid in organic synthesis [8]. Advantages stem amongst others form the high surface area and the wide range of pH stability of activated carbon. It is appeared from our previous study that supported ZS on activated carbon owed excellent catalytic activity for esterification of acrylic acid [9]. However, little knowledge on the catalytic activity of long chain carboxylic acid, such as fatty acids.

We report here the results on the esterification of fatty acid catalyzed by ZS supported on activated carbon. The studies were performed in batch reaction under solvent-free condition, and the catalytic activity performance of the catalysts was compared to that of conventional resins. In addition, we have conducted XRD, nitrogen adsorption, and XPS investigation to determine the properties of the catalysts.

2. Experimental

2.1. Materials

Zirconium sulfate [$Zr(SO_4)_2 \cdot 4H_2O$], oleic acid and *n*-butanol were of AR grade purchased from Beijing

*To whom correspondence should be addressed.
E-mail: zhangjc1@mail.buct.edu.cn

Shiji Chemical Co. The activated carbon used was from Guanghuajingke Chemical Co., Beijing China. An average particles size from 60 to 80 mesh of activated carbon was used, in order to exclude internal diffusion. Zeolite types solid acid, such as H-Y (Si/Al = 4), HZSM-5 (Si/Al = 38), Hβ (Si/Al = 8), and H-mordenite (Si/Al = 5) were obtained form commercial sources. The Amberlyst-15 resins and Nafion-H (NR 50, 7–8 mesh) were purchased from Sigma-Aldrich Inc.

2.2. Catalyst preparation

The desired amount of ZS in aqueous solution was impregnated on activated carbon. The activated carbon was pretreated under vacuum to evacuate the pores before impregnated with ZS. The suspension was stirred overnight at room temperature. After drying, the prepared catalysts were calcined at 160 °C and denoted by their weight percentage of ZS. For instance, 10% ZS/AC indicates the catalysts containing 10 wt.% ZS.

2.3. Characterization

2.3.1. X-ray powder diffraction measurement

X-ray diffraction was performed on a Shimadzu HR 6000X. The conditions used were: Cu Kα radiation (λ = 1.54056 Å) at 40 kV and 200 mA, scanning angle (2θ) from 5 to 60° with scan-steps of 0.04° per second.

2.3.2. Textural properties

The textural properties were performed on Micromeritics ASAP 2010 model instrument from the nitrogen adsorption isotherms at 77 K. All samples were degassed at 100 °C under vacuum for 8 h. Specific surface area (S_{BET}) were calculated from the linear part by BET equation. The total pore volume (V_{total}), which represents the volume of micro- and mesopores, was determined at relative pressure of 0.95 [10]. The Horvath–Kawazoe model was used to calculate micropores volume (V_{micro}) and micropores size (D_{micro}). Consequently, the mesopore volume (V_{meso}) was calculated by subtracting the value of V_{total} from amount of adsorbed at P/P_o = 0.95, $V_{total}-V_{micro}$ [11]. The mesopore size (D_{meso}) distribution was determined by BJH theory, which provided in the manufacturer software.

2.3.3. XPS analysis

X-ray Photoelectron spectra (XPS) were acquired with an Escalab 250 (ThermoVG) spectrometer equipped with a hemispherical electron analyzer and Mg Kα (hv 12536 eV, 1 eV = 1.6302×10^{-19} J) 120 W X-ray source. The powder samples were pressed into small Inox cylinders and then mounted on a heater placed in a pretreatment chamber of the instrument, were evacuated in the pretreatment chamber for overnight. The residual pressure of the ion-pumped analysis chamber was maintained below 5×10^{-9} Torr during data acquisition. The binding energy of adventitious carbon 1s core level, which is 284.8 eV, was used to correct the energy shift due to surface charging.

2.3.4. Esterification of oleic acid with n-butanol

Esterification reaction was performed in three-neck flask at atmospheric pressure equipped with a telfon-coated magnetic stirring bar, a thermometer, Dean-Strak receiver and reflux condenser. A typical esterification reactant consists of oleic acid (31.6 mL, 0.10 moles), *n*-butanol (11.0 mL, 0.12 moles) and fresh catalyst (1.41 g). The moles ratio for oleic acid to *n*-butanol is 1:1.2 and the weight ratio of the catalyst was 5 wt.%, based on oleic acid. The reaction temperature was slowly raised to 110–120 °C and maintained at the desired temperature during the specified reaction periods. The conversion was determined with a gas chromatography (FID-GC, Shimadzu GC-8A) using a column of crossbonded 100% dimethyl polysiloxane (15 m) and tetradecane as internal standard. The parameter for the temperature program; start at 150 °C (2 min), ramp at 5 °C min^{-1} to 250 °C.

3. Results and discussion

3.1. Characterization of the catalyst

3.1.1. XRD

XRD patterns of ZS/AC at different loadings are shown in figure 1. It was observed that ZS was well-dispersed on AC surface, because no diffraction lines corresponding to bulk ZS were observed up to 40 wt.% loading. This can be seen from figure 1(g), where the ZS diffraction line is clearly observed in a physical mix of ZS with AC. The physical mix gave obvious reflections corresponded to bulk ZS. This result is not surprising because physically mixed ZS tends to agglomerate

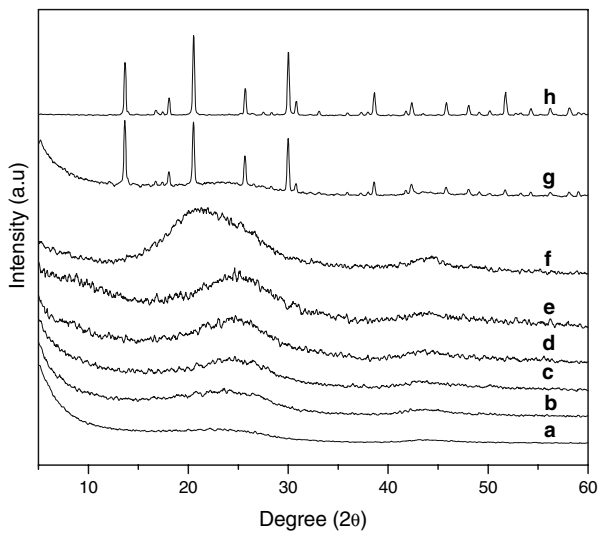

Figure 1. XRD patterns for (a) AC, (b) 10% ZS/AC, (c) 20% ZS/AC, (d) 30% ZS/AC, (e) 40% ZS/AC, (f) 10% ZS/AC reused, (g) physical mix of 10 wt.% ZS with AC, and (h) pure ZS.

compared to a well-dispersed ZS in an aqueous solution. The diffraction patterns of AC structure could still be observed after impregnation. It is interesting to note that broad peak intensity center at $2\theta = 25.1°$ is more striking, as the loading increase. It is suggested that the rise of the broad peak is corresponding to the reflection of ZS. Although the broad peak become more striking as the loading increase, the sharp reflection peak corresponded to bulk ZS is not observed. These results lead us to believe that the ZS is still well-dispersed on AC. As shown in figure 1(f), the carbon supported ZS catalyst did not exhibit sharp peak corresponded to bulk ZS after it was recycled for fourth times. If sintering or agglomeration of ZS occurred, the sharp reflection peaks corresponded to bulk ZS could be clearly observed. It is suggested that during fourth time of reuse, the ZS is still finely dispersed on AC.

3.1.2. Surface area and porosity

As shown in table 1, the reduction in BET surface and total pore volumes with impregnation is mainly due to deposition of ZS on mesopores. The ratio of meso/micro-porosity volumes decreased with the impregnation demonstrating that the amount of ZS deposited on mesopores was more than that deposited in micropores. This result is expected because ZS tends to deposit on the bigger pores before entering the smaller pores. On the other hand, the microcrystalline size of ZS is small and readily located inside the pores of AC. It is shown that the meso- and micropores sizes did not critically reduce after impregnating with ZS. Therefore, we can assume that ZS is finely deposited inside the pores of AC. Although the surface area of support has reduced after impregnation, the carbon-supported ZS still owed higher surface area than that of bulk ZS.

3.1.3. XPS spectra of ZS/AC

To study the surface properties of the supported ZS, we have carried out XPS analysis. Figure 2 shows XPS spectra of Zr_{3d}, S_{2p}, and O_{1s} region in pure ZS and ZS/AC. This clearly indicated that ZS species have been successfully impregnated on AC. Although the binding energy for Zr_{3d} was slightly shifted to higher energy levels in ZS/AC, there were no significant changes observed for S_{2p} and O_{1s}. In addition, the intensity of there three element was also not significantly effected. If there is a change in the intensity, it is due to the (i) presence of more than one type of species with different

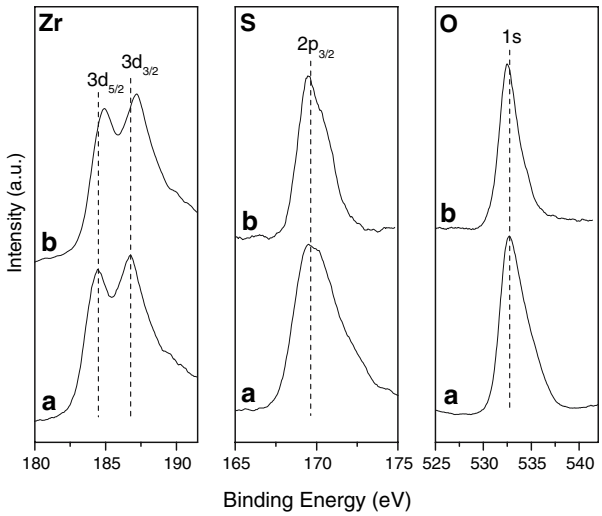

Figure 2. XPS spectra of (a) ZS and (b) 10% ZS/AC at Zr_{3d}, S_{2p}, and O_{1s} binding energy region.

chemical characteristics, or (ii) electron transfer between ZS and the support. Therefore, it is observed that the chemical environment of Zr atom has changed after supported on AC. These results lead us to assume that there is only weak coulombic interaction between ZS species and AC.

3.2. Catalytic activity of the catalyst for esterification of oleic acid

3.2.1. Effect of ZS loading on AC

Figure 3 presents the change of the conversion in the esterification of oleic acid as a function of the ZS loading. It is noteworthy that catalytic activity of supported ZS is better than that of parent ZS. In term of turn over frequency, the 10% ZS/AC is around 10 times more active than that of parent ZS. This result was not surprising because the well-dispersion of ZS on AC has contributed to a higher catalytic activity. The conversion of oleic acid increase rapidly in the 5 wt.% and gradually level off after more than 10 wt.% loading. Further, upon loading the ZS to above 30 wt.%, the conversion gradually decreased. For example, a 84% conversion obtained at 5 wt.% to level off around 88% at 10 wt.% loading; on increasing the loading to 40 wt.%, the conversion deceased to 85%. This is explained by the deceased of surface area at a higher loading. The surface area analysis revealed that ZS is finely dispersed on AC

Table 1
Textural properties of the catalyst at various loading

Sample	S_{BET} ($m^2\ g^{-1}$)	Pore volume (mL g^{-1})			V_{meso}	D_{micro} (nm)	D_{meso} (nm)
		V_{total}	V_{micro}	V_{meso}	V_{micro}		
Activated carbon (AC)	1000	1.01	0.64	0.37	0.6	1.0	5.7
10% ZS/AC	861	0.87	0.62	0.25	0.4	1.0	5.5
40% ZS/AC	232	0.23	0.18	0.05	0.3	1.0	5.4

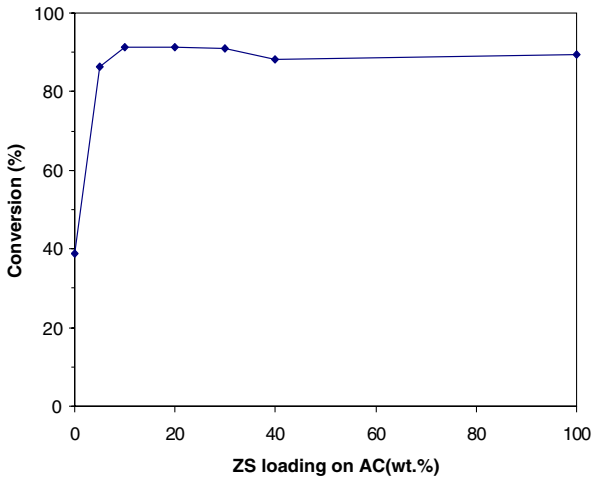

Figure 3. Catalytic activities of ZS loading on AC for esterification of oleic acid.

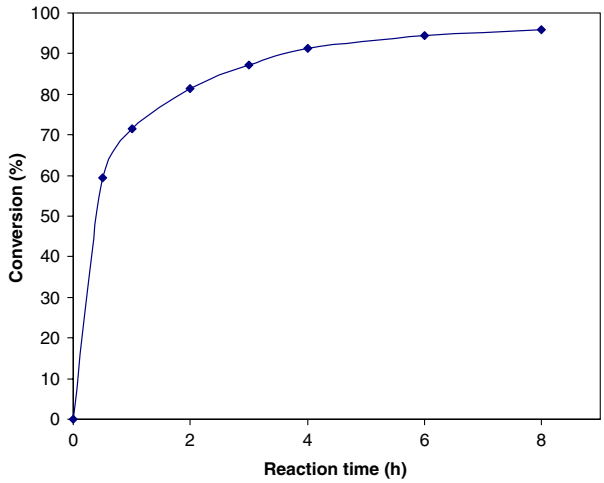

Figure 4. Effect of time over 10% ZS/AC for esterification of oleic acid.

but the surface area is dramatically decreased upon loading the ZS to 40 wt.%.

3.2.2. *Effect of reaction time*

The effect of reaction period on the esterification was studied on 10% ZS/AC. The reaction was carried out without using any extra solvent, such as toluene to promote more environmentally friendly reaction. It is found that azeotropic distillation is also possible with some excess of *n*-butanol. After condensation, water separated from the organic phase, which was then recycled back to the reaction. Although, there is no doubt, the conversion will keep increasing after 4 h toward completion, but due to industrial concern, a rapid production is substantial for economical benefit. Therefore, if esterification reaction takes more time, the catalyst is considered extravagant to be used in industry. Figure 4 show the conversion of oleic acid increases rapidly in the beginning and gradually levels off after 4 h. In addition, the selectivity of the product remains at above 99%. For instance, the conversion from around 59% in the first 30 min to around 87% in 3 h; on increasing the reaction time to 4 h, the conversion increased only to 91%.

3.2.3. *Reusability*

In order to examine the life cycle and reusability of supported ZS, it was repeatedly served for butyl oleate synthesis. The catalyst was filtrated and reused in a new reaction cycle without any treatment, such as calcination or washing. Figure 5 shows the results obtained for the usage of the same catalyst in several cycles. It is observed from the graph that there was a slight decrease of the activity when the catalyst was reused. However, the reusability of the supported ZS is better than that of parent ZS. Indeed, there is an encapsulation of the ZS by the carbon. We have determined the quantity of the ZS in the solution after filtration by using inductively coupled plasma-optical emission spectroscopy (ICP-OES). However, there is no Zr elements was detected during first, second, third and fourth time of reuse. It is shown that the leaching of ZS during reaction cannot explain the size of the activity decrease. A more reasonable explanation might be due to blocking of the active sites. Further, we have carried out the reaction of the reused catalyst after it was washed with dichloromethane. The conversion of oleic acid was improved to 80% after the catalyst was washed. It is assumed that blocking of active sites is more pronounced.

3.2.4. *Effect of catalyst loading and reactants mol ratio*

It is not of practical interest to use large amount of catalyst, and more over the removal of adsorbed high molecular weight products, such as butyl oleate from the

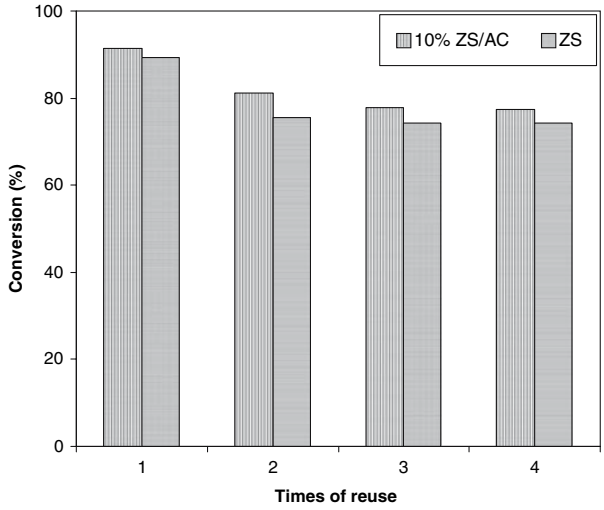

Figure 5. Reusability of catalytic activity of ZS and 10% ZS/AC catalyst in the esterification of oleic acid.

catalyst is expensive. Hence, optimizing catalyst loading based on limiting reactant was studied. The effect of the catalyst loading over the conversion is presented in table 2 (entries 1–4). It can be observed that the conversion of oleic acid was increased by increasing the catalyst amount. This finding is expected because catalyst loading increment proportional to availability of acid sites, which favor the accessibility of large number of reactant to catalyst active sites. There is no significantly catalytic enhancement can be achieved after 5 wt.% of catalyst loading.

As shown in table 2 (entries 4–8), the effect of mole ratio of oleic acid to *n*-butanol was varied from 1 to 2.6, while keeping the other experimental conditions constant. The *n*-butanol is excess because it is more economical than oleic acid. The mole ratio of oleic acid:*n*-butanol was varied as 1:1.0, 1:1.2, 1:1.4, 1:1.8, and 1:2.6. The conversion of oleic acid increased as the molar ratio increased. The excess amount of the reactant *n*-butanol shifted the equilibrium to the product side thus increased the conversion. However, the conversion of oleic acid increases rapidly in the 1:1.2 mol ratio and gradually levels off after more than 1:1.4 mol ratio. For example, a 78% conversion obtained at 1:1.0 mol ratios to around 91% at 1:1.2 mol ratios; on increasing the mol ratio to 1:1.4, the conversion increased only to 94%. Meanwhile, further increase of mol ratio to 1:1.8, the conversion beginning to decrease. Besides the excess of the reactant shifted the equilibrium, the higher conversion could be attributed to occupancy of the acid over the active sites and the availability of alcohol molecules for further esterification. In the other hand, the effect of mole ratio over the conversion can be attributed with the occupancy of acids over the active sites and availability of alcohol molecules for further esterification [12,13]. It is well agreed with the literatures reported earlier [12,13], it is assumed at a mole ratio 1:1.0 that the fatty acid is chemisorbed on the active sites to form carbonium ions. The attack of these stable carbo cations by the alcohol to form esters is least effective in the 1:1.0 ratio stages. Further, when the concentration of alcohol is excess, the approach of *n*-butanol molecules to the carbo cation is to be enhanced showing an increase in conversion. The decreased in conversion with increased in the mol ratio to 1:1.8 was due to the flooding of active sites with alcohols molecules rather than oleic acids. Therefore, increase of alcohols mole ratio hindrance the completion of oleic acid being protonated at the active sites. This indirectly proved that Eley-Rideal mechanism with chemisorption of oleic acid on the active sites to form carbo cation.

Table 2
Effect of amount of catalyst and feed mol ratio on esterification of oleic acid over 10% ZS/AC[a]

Entry	Oleic acid:*n*-butanol (mol ratio)	Catalyst amount (wt.%)	Conversion (%)
1	1:1.2	3	82.5
2	1:1.2	4	84.1
3	1:1.2	5	91.3
4	1:1.2	6	92.1
5	1:1.0	5	77.9
6	1:1.4	5	93.7
7	1:1.8	5	90.4
8	1:2.6	5	76.3

[a] Reaction conditions: substrates: oleic acid (0.1 mol), *n*-butanol (0.12 mol); catalysts: 5 wt.% based on fatty acid; reaction temperature: 120 °C; reaction time: 4 h.

Table 3
A comparison of esterification of oleic acid over 10% ZS/AC with other solid acid catalysts[a]

Solid acids	Conversion (%)
HZSM-5 (Si/Al = 38)	39.1
HY (Si/Al = 4)	39.6
Hβ (Si/Al = 8)	41.8
H-mordenite (Si/Al = 5)	38.3
Nafion-H	37.5
Amberlyst-15	87.9
10% ZS/AC	91.3
Without catalyst	36.3

[a] Reaction conditions: substrates: oleic acid (0.1 mol), *n*-butanol (0.12 mol); catalysts: 5 wt.% based on fatty acid; reaction temperature: 120 °C; reaction time: 4 h.

3.2.5. *Comparison with different solid acids*

Table 3 show the influence of various solid acids on the conversion of oleic acid. The zeolite types catalyst, such as HZSM-5, HY, Hβ, and H-mordenite exhibit low conversion because the reactant cannot make its entry easy into the pores of zeolites. It is noteworthy that the small pores obstruct the entry of the bulky organic molecules reactant, such as oleic acid into the pores. This phenomenon is also observed in Nafion-H, where the reactant is hardly make it way into the actives sites. Acidic resins, such as Amberlyst-15 are known to be very efficient catalyst for esterification reaction and even some of them are commonly used in industrially. Unfortunately, the acidic resin easily deactivated upon heating up to 120 °C for long period [3]. It is evident from these data that conversion of oleic acid with ZS/AC catalyst is higher than that of acidic resin and other solid acid catalysts.

4. Conclusion

We have shown that ZS/AC is an efficient catalyst for the esterification of oleic acid by *n*-butanol. The catalytic activity of supported ZS is higher than that of parent ZS and even higher that of conventional acidic resins. However, deactivation if the catalyst occurs in the batch reaction during four times of reuse. The high catalytic activity of the supported catalyst are due to the

well-dispersion and larger surface area. It was noteworthy that esterification of fatty acid could be carried out at low reaction period and low amount of catalyst under solvent-free condition to promote greener reaction.

Acknowledgments

The authors are thankful to the National Natural Science Foundation of China (No. 20076004) and Malaysia Ministry of Science and Technology (IRPA grant 09-02-02-0033) for the financial support. We are also grateful to UNESCO/China Great Wall Co-Sponsored program for a fellowship to J.C. Juan.

References

[1] K. Mantri, K. Komura and Y. Sugi, Green Chem. 7 (2005) 677.
[2] K. Wilson and J.H. Clark, Pure Appl. Chem. Vol. 72 (2000) 1313.
[3] J.C. Juan, J.C. Zhang and M.A. Yarmo, J. Mol. Catal. A: Chem. 267 (2007) 265.
[4] W. Cao, J. Zhang and Q. Lv, J. Petrochem. Univ. 13 (2000) 41.
[5] W. Cao, J. Zhang and Q. Lv, J. Beijing Univ. Chem. Tech. 26 (1999) 72.
[6] J.C. Juan, Y. Jiang, X. Meng, W. Cao, M.A. Yarmo, J.C. Zhang, Mater. Res. Bull. xxx (2006) xxx–xxx. (in press).
[7] D. Richard and P. Gallezot, *Preparation of Catalysts IV*, (Elsevier, Amsterdam, 1987) 71.
[8] M.E. Chimienti, L.R. Pizzio, C.V. Caceres and M.N. Blanco, Appl. Catal. A: Gen. 208 (2001) 7.
[9] J.C. Zhang, X. Meng and W. Cao, Chinese J. Catal. 27 (2006) 135.
[10] K. Gergova and S. Eser, Carbon 34(7) (1996) 879.
[11] F. Rodriguez-Reinoso, M. Molina-Sabio and M.T. Gonzalez, Carbon 33(1) (1995) 15.
[12] B.R. Jermy and A. Pandurangan, J. Mol. Catal. A: Chem. 237 (2005) 146.
[13] R.K. Sharath, N. Nagaraju and K.V.R. Chary, Appl. Catal. A: Gen. 299 (2006) 185.